ORIGINAL PAPER

Investigation into mechanisms and kinetics of asphaltene aggregation in toluene/*n*-hexane mixtures

Bahram Soltani Soulgani[1] · Fatemeh Reisi[1] · Fatemeh Norouzi[1]

Abstract
Determining the rate of asphaltene particle growth is one of the main problems in modeling of asphaltene precipitation and deposition. In this paper, the kinetics of asphaltene aggregation under different precipitant concentrations have been studied. The image processing method was performed on the digital photographs that were taken by a microscope as a function of time to determine the asphaltene aggregation growth mechanisms. The results of image processing by MATLAB software revealed that the growth of asphaltene aggregates is strongly a function of time. Different regions could be recognized during asphaltene particle growth including reaction- and diffusion-limited aggregation followed by reaching the maximum asphaltene aggregate size and start of asphaltene settling and the final equilibrium. Modeling has been carried out to predict the growth of asphaltene particle size based on the fractal theory. General equations have been developed for kinetics of asphaltene aggregation for reaction-limited aggregation and diffusion-limited aggregation. The maximum size of asphaltene aggregates and settling time were modeled by using force balance, acting on asphaltene particles. Results of modeling show a good agreement between laboratory measurements and model calculations.

Keywords Asphaltene precipitation · Kinetic modeling · Diffusion-limited aggregation (DLA) · Image processing · Asphaltene aggregation

1 Introduction

Asphaltenes are complex fractions in petroleum fluids, with variations of molecular weight, structures and polarity (Speight 2014). Asphaltenes are polyaromatic structures or molecules that contain heteroatoms such as oxygen, sulfur and nitrogen and metal elements including Ni and V, which are in an aggregation state in petroleum (Civan 2015). Asphaltenes are poorly defined as solubility class which are dissolved in toluene and insoluble in normal alkane such as *n*-hexane (Yarranton and Masliyah 1996). Any change in thermodynamic conditions such as pressure, temperature or composition may render asphaltenes from solution and cause to asphaltene precipitation (Andersen and Stenby 1996). Asphaltenes may precipitate in reservoirs, near the

wellbore, tubing, pipeline transport and process facilities in downstream (Kokal and Sayegh 1995). Asphaltene deposition in reservoirs reduces the rock permeability dramatically and even may plug the pores completely (Soulgani et al. 2011; Kord et al. 2014). In addition to formation damage, asphaltene deposition in the tubing and pipelines reduces the available diameter of the pipe to flow that decreases the oil production capacities (Soulgani et al. 2009). Precipitated asphaltene particles tend to stick together and form aggregates due to molecular forces. In this case, the large particles may settle down as deposits and sediments on the surface of solids. This solid surface may be a pore surface in reservoirs, surfaces of tubing and pipes, production vessels or any other part of process facilities that fluids pass through them. Although several different methods are available to remove asphaltenes such as chemical or mechanical, these methods are very expensive and also take long time to remove asphaltenes completely. Therefore, it is better to prevent asphaltene deposition by understanding the mechanisms of asphaltene aggregation. Because settling and deposition of asphaltenes occur by forming large aggregates of asphaltenes in oil that can be modeled by studying the

Edited by Yan-Hua Sun

✉ Bahram Soltani Soulgani
  Soltani.b@put.ac.ir

1 Department of Petroleum Engineering, Petroleum University of Technology, Ahwaz, Khouzestan, Iran

mechanisms of aggregation, it is vital to study the asphaltene aggregation behavior in order to find an effective solution to prevent or mitigate the severity of asphaltene problems. Numerous studies have been carried out to investigate the kinetics of colloidal aggregation of different solid particles (Schaefer et al. 1984; Weitz and Oliveria 1984; Sheu et al. 1992; Mozaffarian et al. 1997; Sun et al. 2017; Maqbool et al. 2011; Haji-Akbari et al. 2015; Mohammadi et al. 2016).

Yudin et al. (1998a) applied the Derjaguin–Landau–Verwey–Overbeek (DLVO) theory to explain asphaltene aggregation behavior. The DLVO theory which explains the colloidal stability was developed by Derjaguin and Landau and Verwey and Overbeek. The theory explains the tendency of two particles due to potential energies of attraction (London–van der Waals) and repulsive electrostatic versus interparticle distance. When the concentration of asphaltenes in the solution is high, the van der Waals force is dominant and unstable colloidal particles of asphaltene attract each other and form an aggregate. As the concentration of asphaltenes in the solution decreases, the distance between the aggregate particles increases, which reduces the attractive force, and as a result, a stable colloidal solution of aggregates is formed (Schramm 2014).

Kinetics of asphaltene aggregation was described by two different mechanisms which include reaction-limited aggregation (RLA) and diffusion-limited aggregation (DLA). The kinetics of asphaltene aggregation depends on the required time for two asphaltene particles to diffuse and reach to each other and the time that takes for particles to react with each other and form larger particles. In RLA, the reaction rate controls the aggregation process. Because the rate of reaction is slower than the diffusion rate (Lin et al. 1990), in RLA sticking does not occur in each collision between asphaltene particles. In DLA, the diffusion rate controls the aggregation process. Hence, during the DLA mechanism, the reaction of forming aggregates is fast, and as a result, asphaltene particles stick together in each contact (Yudin et al. 1998b).

Rastegari et al. (2004) found asphaltene aggregates tend to be loose fractal-like rather than dense aggregates and applied a fractal model to predict the growth of the mean particle diameter.

Hung et al. (2005) introduced the equations for the particle growth in RLA and DLA as follows:

$$R = R_0 \exp\left(t/\tau_R d_f\right) \tag{1}$$

$$R = R_0\left(1 + t/\tau_D\right)^{\frac{1}{d_f}} \tag{2}$$

where R is the mean radius of asphaltene particles in any time, R_0 is the initial mean radius of particles, d_f is the fractal dimensionality, t is the time and τ_R and τ_D are the reaction and diffusion time, respectively. d_f, τ_R and τ_D are adjustable parameters that should be fitted by the result of particle size analysis of the experimental data. Seifried et al. (2013) also studied the mechanisms of asphaltene aggregation by the RLA and DLA formula for different precipitants and solvents.

The problem of Eqs. (1) and (2) is that their coefficients should be tuned for each concentration of asphaltene, solvent and precipitant. Therefore, extensive experiments should be carried out to obtain experimental data for each specific concentration of asphaltene solution and precipitant. Hence, to resolve this problem, it was necessary to develop general equations to cover all concentrations. In order to find the general form of equations, extensive experiments on the solution of asphaltenes in toluene with different concentrations of n-hexane have been conducted. Asphaltene aggregation has been studied using a high-resolution microscope to determine the diameter of asphaltene particles. This method is excellent, because it has no direct interaction with asphaltene particles which can affect the aggregation growth process. It was followed by image processing to find the distribution of asphaltene particles and calculate their mean aggregate diameter.

In this paper, based on extensive experiments, general equations will be presented to cover the full range of asphaltene aggregation. In addition, hydrodynamic modeling has been carried out to determine the critical size of precipitating asphaltene particles using force balance acting on suspended particles. The developed equations are used successfully to predict the different asphaltene precipitation criteria, including the mean particle size and exact time of deposited asphaltene aggregates.

2 Asphaltene particle size and precipitation experiments

2.1 Experimental materials

The asphaltenes were extracted from one of the Iranian crude oils with a density of 0.890 g/cm^3, viscosity of 392.6 cp (at 15.6 °C) and 8.1% asphaltene content based on IP143 standard. In addition to remove the effects of the other crude oil components, crude oil was very dark. Therefore, it was not possible to conduct a visual study to measure the size of asphaltene aggregates, so diluted solutions have been prepared. The asphaltene was separated from crude oil and weighted accurately and then was dissolved in a specified volume of toluene as a base solution. After that, different volumes of n-hexane were added to the solution. Toluene (as solvent) and n-hexane (as precipitant) used for all experiments were obtained from Merck Company with purity of 99.9 and 99 percent, respectively.

2.2 Experimental methods

In order to remove interaction effects between asphaltene aggregates and other crude oil components, asphaltenes were separated from crude oil. Then, asphaltenes were dissolved in toluene to observe the kinetics of asphaltene aggregation and investigate the stability of asphaltenes at different precipitant concentrations. Initially, the weight of asphaltenes was measured and then dissolved in a specified volume of toluene. After that, different volumes of *n*-hexane were added to the solution as precipitant agent for destabilizing the dissolved asphaltenes. In order to study the growth of asphaltene particles, it is necessary to determine the onset of asphaltene precipitation. In this paper, the onset of asphaltene precipitation was determined using the filtration method. In this method, different concentrations of *n*-hexane were added to the dissolved asphaltenes in toluene and passed through a 0.5-μm filter. Remained asphaltenes on the filter paper were measured, and the onset of asphaltene precipitation was determined. Asphaltenes were unstable in a solution with *n*-hexane concentration above the onset of asphaltene precipitation. In all experiments, 0.02 g of asphaltenes and 1.5 mL of toluene as solvent were used. In order to study the asphaltene aggregation growth, a special cell was designed and made by glass that is shown in Fig. 1. As could be seen, the cell was cylindrical in shape with a diameter of 5 mm and a height of 100 μm that was made using laser cutting followed by washing with hydrofluoric
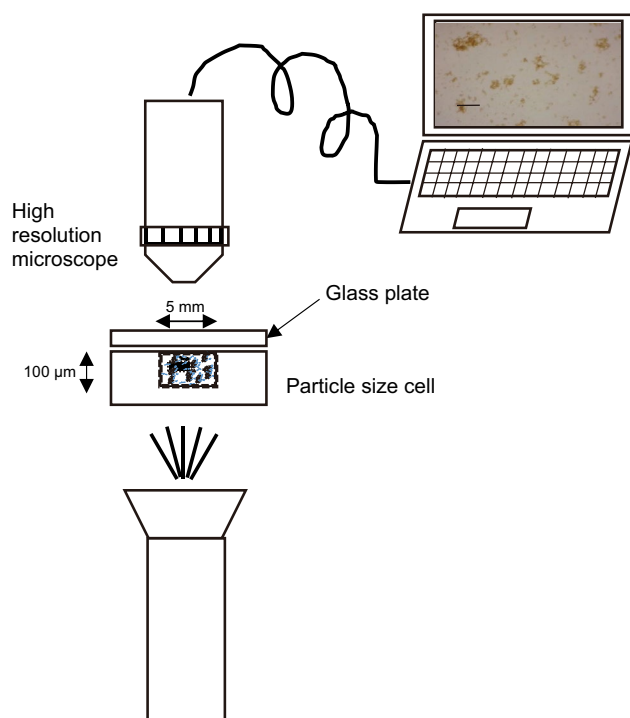

Fig. 1 Experimental setup for particle size study

acid. The cell size has been chosen to allow free movement of asphaltene particles during the tests. A glass plate covers the cell to seal the experimental solution and to prevent vaporization of toluene and *n*-hexane mixture. Therefore, the concentrations of solvent and solute remain constant during the tests. The experiment container was fixed in order to let the asphaltenes deposit.

The *n*-hexane was added to the solution in different concentrations starting from 0.7 to 1.1 mL in the separate closed test tube. The experiments were carried out under ambient pressure and room temperature. Kinetics of asphaltene aggregation experiments were started immediately after adding *n*-hexane. Nevertheless, zero time ($t = 0$ min) was defined when visual observation of the sample with the microscope was started.

Samples were transferred to the particle size cell. A Dino-Lite microscope was used to take photographs and capture them by its software for every 10 min. The photographs were taken at different times and processed to determine the size of asphaltene aggregates. Experiments were continued until there was no significant increase in the size of asphaltene aggregates observed.

Photographs were processed by image processing program in MATLAB software in order to get the most accurate and reliable results. Distribution of asphaltene aggregate size and frequency of them were obtained by image processing analysis. In order to check the validity and also the repeatability of tests, the particle size analysis was conducted for the same solution with a ZEN 3600 particle size analyzer (Malvern, UK). Results were in excellent agreement with visual image processing analysis.

3 Experimental results

In order to study the effect of asphaltene concentration, different solutions were prepared. The base solution consisted of 0.02 g of asphaltenes that were dissolved in 1.5 mL of toluene. This solution was used as based in all experiments. The onset of asphaltene precipitation by adding *n*-hexane as precipitant was determined by the filtration method. The onset of asphaltene aggregation in toluene solution was determined at 29 vol% of *n*-hexane concentration. Then, *n*-hexane was added to the base solution in different test tubes above the asphaltene onset with different volume percentages of *n*-hexane including 32, 38, 40 and 42.

Taking photographs was started immediately after transferring samples to the experimental cell. The growth of asphaltene aggregates was quite clear with respect to the time and changing the concentration of unstable asphaltene. Figure 2 shows the experimental results that 38 vol% of *n*-hexane was added to the asphaltene–toluene solution. Each photograph captures small part of samples. In order
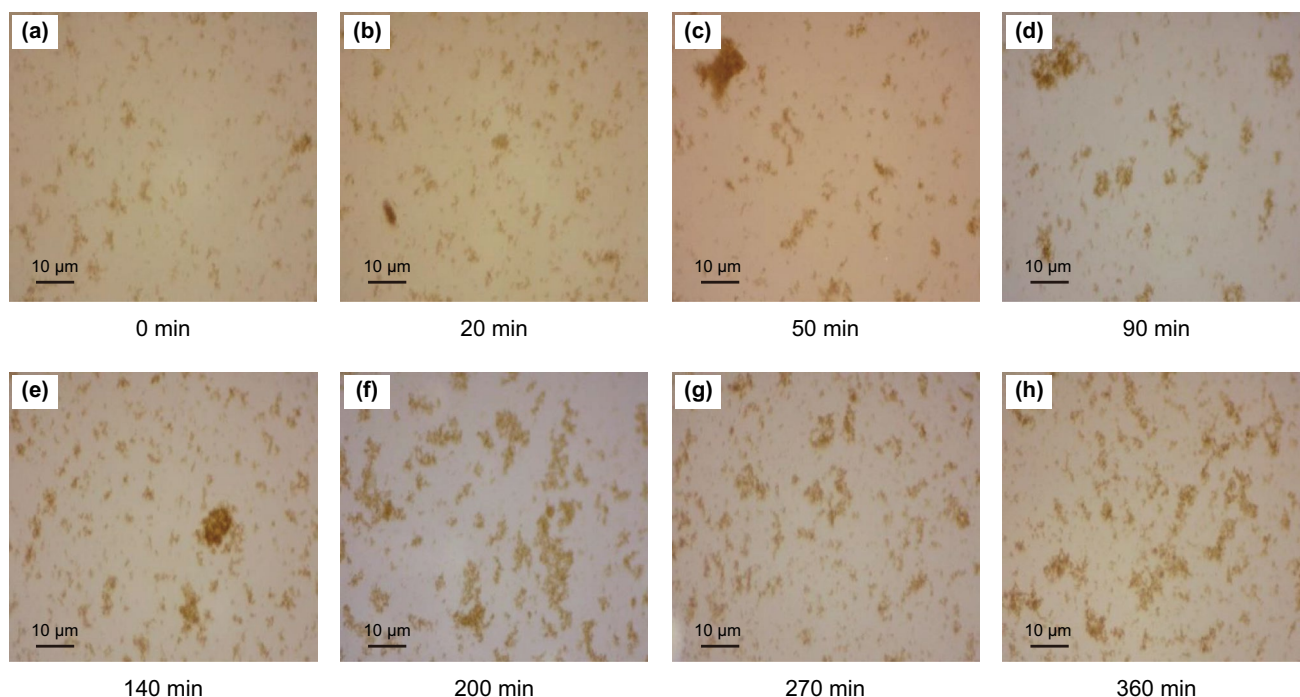
Fig. 2 Images of the asphaltene aggregates in the solution with 38 vol% of *n*-hexane at different flocculation times

to reduce the uncertainties in the analysis of the images, several photographs were taken from different parts of each sample. The average of several photographs was considered as results of particle size analysis for each sample.

Figure 2 shows that the number of asphaltene particles that are separated from the solution increases with time. Thus, although asphaltene aggregation by precipitating agent (*n*-hexane) is a fast process, it will take time to reach the final distribution in the size of aggregates. As a result of increasing the number of aggregates, the possibility of collision between particles increases. Asphaltene aggregates in the solution are free to move by Brownian motions. These random free movements may cause collisions between asphaltenes and form larger asphaltene aggregates. Those large asphaltene particles deposit and are removed from the asphaltene–toluene solution. In this case, the concentration of unstable asphaltene aggregates decreases; consequently, the ratio of toluene as a peptizing agent in the solution increases. Therefore, asphaltene particles are surrounded by more toluene molecules that prevent asphaltene aggregation and result in an equilibrium condition. For this reason, no increase in asphaltene particle size is observed during the ASR. It can be also explained by the DLVO theory. As the number of asphaltene particles in the solution decreases, the distance between asphaltene aggregates increases. Therefore, van der Waals attractive force decreases. Meanwhile, toluene molecules around asphaltene particles repel each other. Therefore, the solution reaches equilibrium and no

further increase in particle size is observed. The number of collisions depends on the viscosity of the mixture, density and distribution of particle sizes. Hence, the kinetics of asphaltene aggregation is different for each concentration of *n*-hexane.

Increasing the size of asphaltene aggregates was studied by analyzing the photographs with image processing technique. The results of the particle size distribution from the start of the experiments are shown in Fig. 3. As could be seen, the distribution of asphaltene aggregates increases up
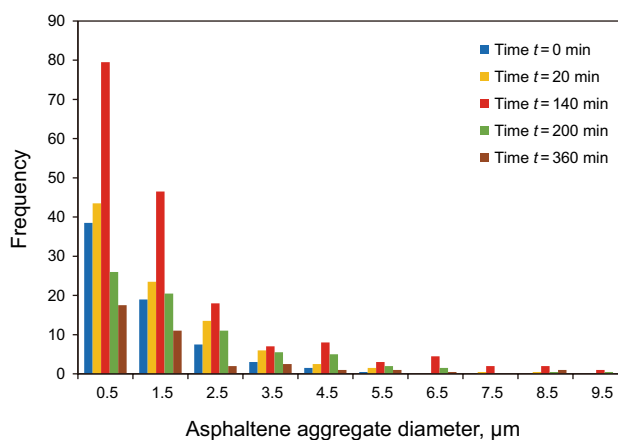

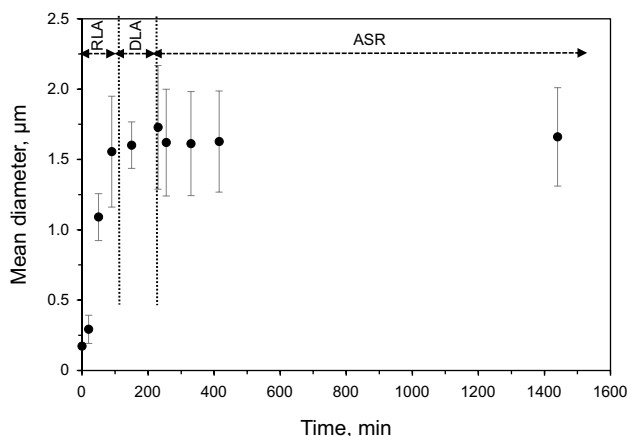**Fig. 3** Asphaltene aggregate diameter distribution for the solution with 40 vol% of *n*-hexane

Fig. 4 Mean asphaltene aggregate diameter versus time

to certain time (in this case 200 min), and after that, the decrease in distribution can be observed.

In the start of the experiment, the majority of asphaltene aggregates are small with sizes less than 4.5 μm. Then, the increase can be seen both in the size and in the cumulative number of asphaltene aggregates. The large aggregates that are formed due to Brownian motion of small aggregates and collision of them are stable in the solution in time less

than 200 min. After that, large aggregates tend to settle to the bottom of the cell. Therefore, the number of large size aggregates and the total cumulative number of aggregates significantly decrease. The mean diameter of asphaltene aggregates is shown in Fig. 4. Experiments were carried out for other concentrations of *n*-hexane including 32 vol%, 38 vol% and 40 vol%. Figures 5 and 6 show the images that have been taken for the solution of asphaltene and toluene with *n*-hexane concentration of 40 vol% and 42 vol%, respectively.

Results of image processing are summarized in Fig. 7. As could be seen, the mean diameter of asphaltene aggregates varies in different concentrations of *n*-hexane. The diameter of asphaltene aggregates increases with increasing the *n*-hexane concentration. However, the time to reach the maximum size of asphaltene aggregates decreases. The dissolved asphaltenes in the solution in high concentrations of *n*-hexane became unstable and came out of the solution. Therefore, the size of asphaltene aggregates is very close to each other in the solutions with 40 vol% and 42 vol% of *n*-hexane. Kinetics of asphaltene aggregation comprises different regions which indicates distinct mechanisms.

Asphaltene aggregation has been explained by Yudin et al. (1998a) with two different mechanisms which were reaction-limited aggregation (RLA) and diffusion-limited
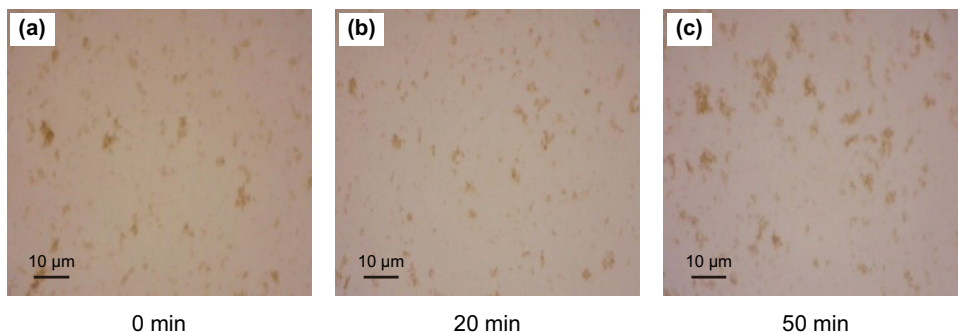

Fig. 5 Images of the asphaltene aggregates in the solution with 40 vol% of *n*-hexane at different flocculation times. **a** 0 min. **b** 20 min. **c** 50 min
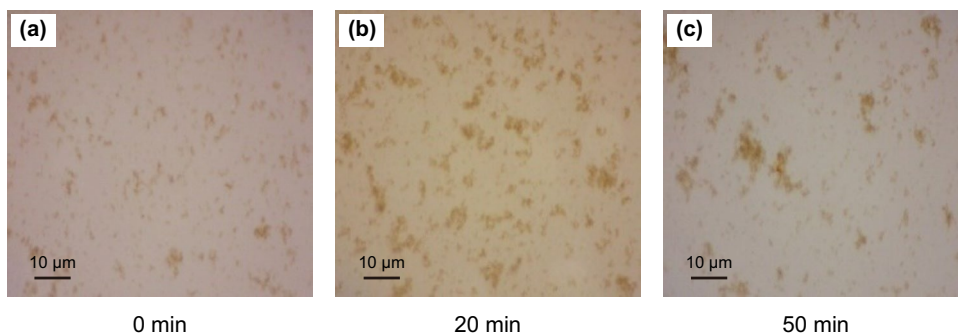

Fig. 6 Images of the asphaltene aggregates in the solution with 42 vol% of *n*-hexane at different flocculation times. **a** 0 min. **b** 20 min. **c** 50 min
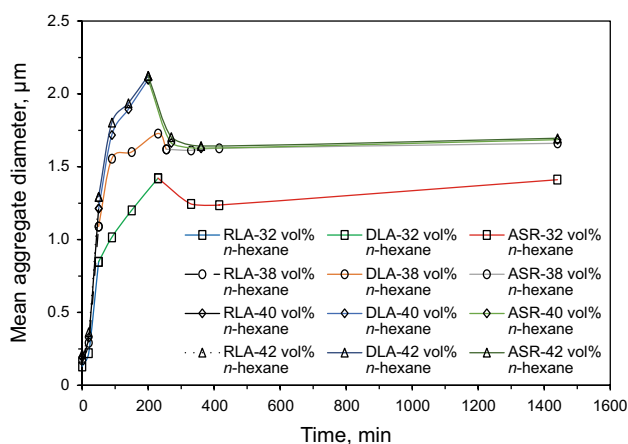
Fig. 7 Mean aggregate diameter versus time in different concentrations of *n*-hexane

aggregation (DLA). Seifried et al. (2013) explained that in DLA each collision results in making larger particles by sticking together. But in RLA the size of aggregates is small and each collision does not necessarily results in the production of larger aggregates. In RLA, the number of asphaltene aggregates in the solution is higher than that in DLA. Although each collision in RLA may not produce the larger particle, due to the greater number of collisions, the growth rate of the aggregate size in RLA is faster than that in DLA. The size of asphaltene aggregates increases in RLA, and this process intensifies in DLA. As could be seen in Fig. 7, the time and the value of maximum asphaltene aggregate size vary in different concentrations of *n*-hexane. The maximum size of asphaltene aggregates in DLA is followed by reduction in the mean particle size. This behavior has been seen in Seifried et al.'s (2013) experiments.

The final region that is shown in Figs. 4 and 7 is what we called it as asphaltene settling region (ASR). In this region, asphaltene aggregates become large enough to separate from the solution and settle as deposits at the bottom of the cell. In this region, the mean size is less than the maximum particle size in DLA and reaches to the final value that varies in different concentrations of *n*-hexane.

4 Asphaltene precipitation modeling

Modeling of asphaltene aggregation is very important for understanding the mechanism of different types of damage caused by asphaltene deposition. Damage may occur by deposition on the surface of pores in reservoirs, the inner surface of tubing and transport pipelines, and in the oil production facilities and refineries equipment.

Therefore, enormous research has been carried out to predict the behavior of asphaltene particles under different

conditions. Kawanaka et al. (1989) presented a thermodynamic model to predict the size distribution of asphaltene particles. Browarzik et al. (1999) modeled the average molar mass of asphaltene in the solutions at equilibrium. Yudin et al. (1998b) introduced two mechanisms, RLA and DLA, for the growth of asphaltene particles that have been used by Hung et al. (2005) and Seifried et al. (2013).

These mechanisms predict asphaltene aggregate size excellent in the presence of *n*-alkanes using Eqs. (1) and (2). There are some parameters in Eqs. (1) and (2) that should be tuned with experimental data, including d_f, τ_R and τ_D. Tuning should be carried out for each concentration of *n*-hexane as precipitant and different values have been reported.

In this paper, general equations are introduced that can include different concentrations of toluene as solvent, asphaltene concentration and *n*-hexane as precipitant:

$$R = R_0 \left(\frac{m_{\mathrm{asph}} + m_{\mathrm{C}_6}}{m_{\mathrm{tol}}} \right)^a \exp\left(t/\tau_R d_f \right) \tag{3}$$

$$R = R_0 \left(\frac{m_{\mathrm{asph}} + m_{\mathrm{C}_6}}{m_{\mathrm{tol}}} \right)^a \left(1 + \frac{t}{\tau_D} \right)^{\frac{1}{d_f}} \tag{4}$$

where m_{asph}, m_{C_6} and m_{tol} are the mass of the dissolved asphaltene, C_6 and toluene, g, and a is a constant.

Equations (3) and (4) are the general form of RLA and DLA equations that can predict kinetics of asphaltene aggregation. Dimensionless factor has been introduced for both equations to tolerate variable concentrations of all constituents that include the mass, g of dissolved asphaltenes, *n*-alkane (here *n*-hexane) as precipitant agent and toluene as solvent. Parameter "a" is power of dimensionless factor that is different for RLA and DLA mechanisms. As denoted, in Eqs. (1) and (2), there are three parameters that should be tuned for each concentration of precipitant. Different values with wide variations have been reported in the literature for tuning parameters (i.e., d_f, τ_R and τ_D).

However, Eqs. (3) and (4) are modified using dimensionless factor and could be used in all concentrations of precipitant in both RLA and DLA mechanisms with constant values of d_f, τ_R and τ_D. Equations (3) and (4) are applied for tests that have been carried out in this paper. The values of different parameters in Eqs. (3) and (4) for RLA and DLA mechanisms are summarized in Table 1.

Figures 8 and 9 show the quality of the match between measured data and values predicted from Eqs. (3) and (4). As could be seen from Fig. 7, in the asphaltene settling region (ASR) which is after DLA, the mean size of asphaltene particles was reduced. So, the maximum size of asphaltene aggregates can be seen in the DLA region. The variation in size is related to random collision of asphaltene aggregates with each other and forming larger aggregates in the DLA region. New

Table 1 Parameters of developed general equations for RLA and DLA mechanisms

	a	R_0	d_f	τ_R	τ_D
Reaction-limited aggregation	1.15	0.41	1.9	20	–
Diffusion-limited aggregation	1.22	0.44	2	–	1.85
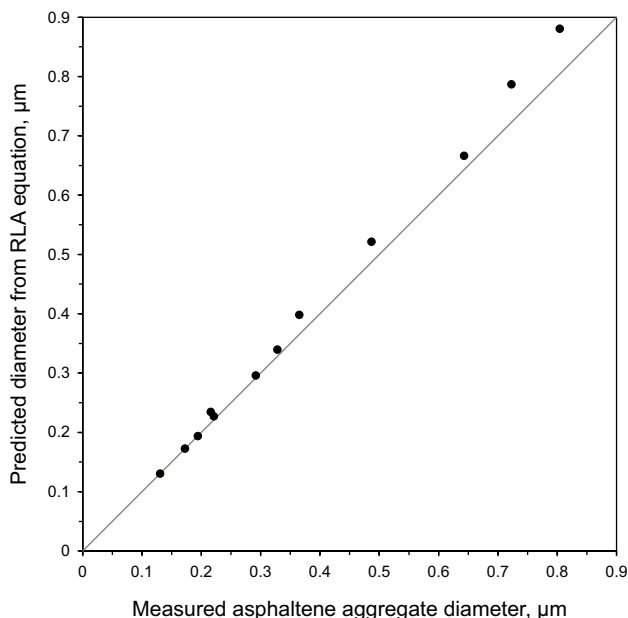
Fig. 8 Comparison of asphaltene aggregate size predicted from general RLA equation with experimental data

Fig. 9 Comparison of asphaltene aggregate size predicted from general DLA equation with experimental data

asphaltene aggregates have greater volume and thereby are heavier. It is the reason that larger aggregates come out of the solution as colloidal particles and settle to the bottom of the cell. Generally, there are three forces acting on each suspended particle, which are gravity, buoyant and drag forces.

The gravity force is applied to the suspended asphaltene aggregates, acting them downward, and the buoyant forces acts upward and the drag force acts in the opposite direction of the motion of asphaltene aggregates.

Settling of asphaltene aggregates as solid layer occurs when the gravity force is more than the summation of buoyant and drag forces. Settling of asphaltene particles depends on the properties of fluid and asphaltene particles including the density and viscosity of fluids and the density, shape and diameter of aggregates.

The buoyant force can be calculated by the following equation (Darby et al. 2001):

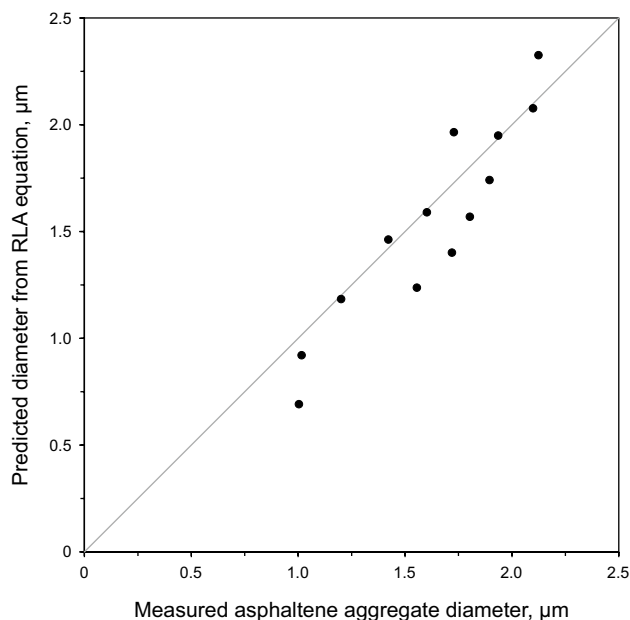$$F_b = \frac{m_a \rho_f g}{\rho_a} = V_a \rho_f g \tag{5}$$

where F_b is the buoyant force, N; m_a is the mass of asphaltene aggregates, kg; ρ_a is the density of asphaltene aggregates, kg/m³; V_a is the asphaltene aggregate volume, m³; and ρ_f is the fluid density, kg/m³; g is the gravity, $g = 9.80665$ m/s². The gravity force that is applied to the body of asphaltene aggregates is equal to:

$$F_g = m_a g \tag{6}$$

where F_g is the gravity force, N.

As mentioned above, drag is acting as an opposite force for deposition of particles which is proportional to the velocity of displacing fluid movement by asphaltene aggregates. When particle moves from its position and falls toward the bottom, it reaches to constant velocity after short time that is called free settling velocity or terminal velocity.

Terminal velocity can be found by wiring the force balance on the asphaltene aggregate particle:

$$F_g = F_b + F_d \tag{7}$$

where F_d is the drag force, N.

Then, by substituting each term of gravity, buoyant and drag forces, Eq. (7) is expressed as:

$$V_a \rho_a g = V_a \rho_f g + \frac{1}{2} C_D \rho_f v_t^2 A_a \tag{8}$$

where C_D is the drag coefficient; v_t is the terminal velocity, m/s; and A_a is the area of asphaltene aggregate. Therefore, the thermal velocity is given by:

$$v_t^2 = \frac{V_a (\rho_a - \rho_f) g}{\frac{1}{2} A_a \rho_f C_D} \tag{9}$$

Drag coefficient for Reynolds less than 1 is given by stock law:

$$C_D = \frac{24}{Re} = \frac{24\mu}{\rho_f v D_p} \tag{10}$$

where Re is the Reynolds number; μ is the fluid viscosity, kg/m s; v is the velocity, m/s; D_p is the particle diameter, m.

As could be seen from Fig. 2, the shape of asphaltene aggregate particles is disk like. Small-angle neutron and X-ray scattering studies also showed the asphaltene aggregates are disk shaped (Eyssautier et al. 2011). Therefore, asphaltene particles are assumed as disk, and by substituting different parameters in Eq. (9) including area and volume of the particle and also drag coefficient, the terminal velocity can be calculated by:

$$v_t = \frac{(\rho_a - \rho_f)g T_a D_a}{12\mu} \tag{11}$$

where D_a is the diameter of asphaltene aggregates, m; and T_a is the thickness of asphaltene aggregate in disk shape, m. Because the size of asphaltene particles is small, Brownian motion is active. The Brownian motion is a random process that causes collisions between small asphaltene aggregates and produces larger aggregates by sticking together. This process continues, and larger aggregates are formed. As long as the size of asphaltene aggregates is small, the buoyant force is more than the gravitational force. As a result, aggregates will be suspended in the solution. However, when the size of aggregates grows sufficiently and larger particles are formed, the gravitational force will be dominant. Hence, heavy aggregates start moving toward the bottom and settle as a solid layer. During this stage, the gravitational, buoyant and drag forces could be calculated by knowing the size of asphaltene aggregates and physical properties of the solution and aggregates. Therefore, the terminal settling velocity of asphaltene aggregates toward the bottom could be determined using Eq. (11). In the experiments that have been presented in this paper, the distance to the bottom of the sample cell was 100 μm. Therefore, the time for asphaltene aggregates to settle at the bottom of the cell was calculated. The calculated time for different sizes of asphaltene aggregates is shown in Fig. 10. As can be seen, modeling of settling time based on balance forces that are acting on asphaltene aggregates achieved excellent prediction for all concentrations of asphaltene solutions. Figure 10 also shows that the rate of asphaltene settling increased with increasing the *n*-hexane concentration as a result of diluting the solution and reduced the viscosity and increased the number of suspended asphaltene aggregates.

It should be mentioned that the settling time also was calculated by assuming the asphaltene particles as
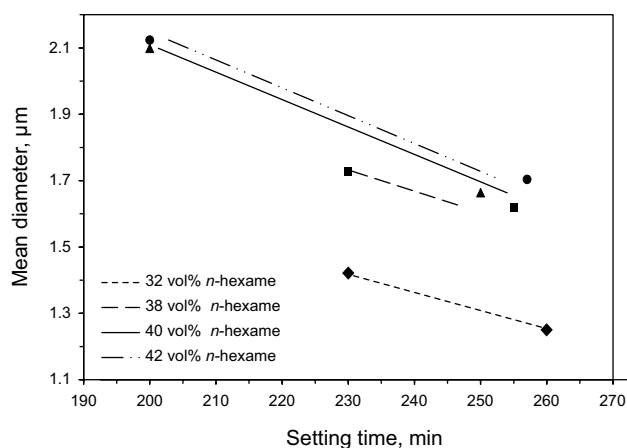

Fig. 10 Modeling of asphaltene aggregation in asphaltene settling region (ASR)

spherical shape. But in this case, the calculated time was less than experimental data which was evidence that asphaltene aggregates are like disk shape. The reason for fast settling was the lower drag force for spherical particles.

Based on the above discussion, now the kinetic behavior of asphaltene particle growth can be explained for asphaltene settling region. Figure 7 shows the maximum size of asphaltene aggregates that are different for each concentration of *n*-hexane as precipitant. It also shows the starting point of the asphaltene settling region (ASR). The maximum size of asphaltene particles that can remain in the solution depends on the properties of asphaltene particles and the solution including density and viscosity. Due to density difference between the fluid and asphaltene particles, some of the asphaltene particles which are larger and heavier settle by gravitational force. Meanwhile, increasing the concentration of *n*-hexane dilutes the solution and reduces the solution viscosity that causes asphaltene aggregates to settle down at different velocities. This is a reason to observe different starting times for each concentration of *n*-hexane in the asphaltene settling region.

Using the force balance equations, the settling time can be estimated as a function of asphaltene aggregate size and other physical properties of the asphaltene particle and the solution including asphaltene density and solution density and viscosity. Figure 11 shows the result of settling time modeling for the 38% *n*-hexane concentration with different sizes of asphaltene aggregates. As can be seen, the asphaltenes with small size need a very long time to settle down. In other words, small particles remain in the solution as suspended particles or in colloidal state and will not deposit. For instance, asphaltene particles with a diameter of 0.1 μm settle after 3985 min, indicating that asphaltene particles of this size will be suspended and will remain in
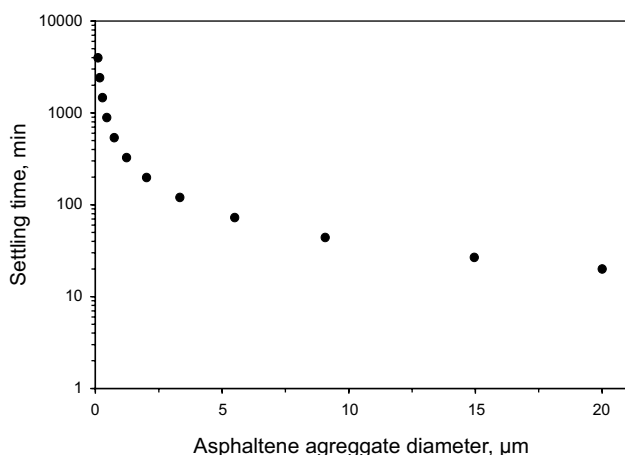
Fig. 11 Modeling of settling time for different asphaltene particle sizes

the solution. However, asphaltene particles with a diameter of 5 μm settle after 79.7 min.

Hence, it is possible to find the maximum size of asphaltene aggregates for each concentration of *n*-hexane or asphaltene content. Image analysis can be used to determine the distribution of asphaltene aggregate sizes. Then, using Eq. (4) which is general form of DLA, the mean average size with respect to the time could be calculated. Force balance could also be utilized to estimate the size of aggregates that are capable of settling. This method can be used to predict the asphaltene particle size to explain the kinetics of asphaltene settling in the ASR region.

5 Conclusions

Kinetics of asphaltene deposition regarding asphaltene aggregation growth is very important to illustrate the state of asphaltene particles. Different mechanisms and behavior can be recognized by the study of asphaltene aggregate size including reaction-limited aggregation (RLA), diffusion-limited aggregation (DLA) and asphaltene settling.

The rate of asphaltene aggregation in RLA is much faster than that in DLA. Large aggregates of asphaltene formed during DLA mechanism settle to the bottom of cell. As a result, the mean average size of asphaltene aggregates decreases in the asphaltene settling region (ASR).

This paper presents a comprehensive study based on extensive experiments that have been carried out to model asphaltene aggregation. General equations have been developed to model kinetics of asphaltene aggregation for both RLA and DLA.

Asphaltene settling region has been studied, and the reduction in the size of asphaltene aggregates has been explained by the balance of three forces enacting upon each suspended asphaltene particle that includes gravity, drag and buoyant forces.

Models were successfully applied to the experimental data, and the size of asphaltene aggregates that could be deposited was calculated. The time of asphaltene deposition for each aggregate size was also calculated. The prediction of depositing time is in excellent agreement with experimental data.

References

Andersen SI, Stenby EI. Thermodynamics of asphaltene precipitation and dissolution investigation of temperature and solvent effects. Fuel Sci Technol Int. 1996;14(1–2):261–87. https://doi.org/10.1080/08843759608947571.

Browarzik D, Laux H, Rahimian I. Asphaltene flocculation in crude oil systems. Fluid Phase Equilib. 1999;154(2):285–300. https://doi.org/10.1016/S0378-3812(98)00434-8.

Civan F. Reservoir Formation damage. Houston: Gulf Professional Publishing; 2015.

Darby R, Chhabra RP, Darby R. Chemical engineering fluid mechanics, revised and expanded. Boca Raton: CRC Press; 2001.

Eyssautier J, Levitz P, Espinat D, Jestin J, Gummel J, Grillo I, et al. Insight into asphaltene nanoaggregate structure inferred by small angle neutron and X-ray scattering. J Phys Chem B. 2011;115(21):6827–37. https://doi.org/10.1021/jp111468d.

Haji-Akbari N, Teeraphapkul P, Balgoa AT, Fogler HS. Effect of n-alkane precipitants on aggregation kinetics of asphaltenes. Energy Fuels. 2015;29(4):2190–6. https://doi.org/10.1021/ef502743g.

Hung J, Castillo J, Reyes A. Kinetics of asphaltene aggregation in toluene–heptane mixtures studied by confocal microscopy. Energy Fuels. 2005;19(3):898–904. https://doi.org/10.1021/ef0497208.

Kawanaka S, Leontaritis KJ, Park SJ, Mansoori GA. Thermodynamic and colloidal models of asphaltene flocculation. In: ACS symposium series. 1155 16Th ST, NW, Washington, DC 20036: American Chemical Society; 1989. Vol. 396, p. 443–458. https://doi.org/10.1021/bk-1989-0396.ch024.

Kokal SL, Sayegh SG. Asphaltenes: the cholesterol of petroleum. In: Middle East oil show, 11–14 March, Bahrain; 1995. https://doi.org/10.2118/29787-MS.

Kord S, Mohammadzadeh O, Miri R, Soulgani BS. Further investigation into the mechanisms of asphaltene deposition and permeability impairment in porous media using a modified analytical model. Fuel. 2014;117:259–68. https://doi.org/10.1016/j.fuel.2013.09.038.

Lin MY, Lindsay HM, Weitz DA, Klein RC, Ball RC, Meakin P. Universal diffusion-limited colloid aggregation. J Phys Condens Matter. 1990;2(13):3093.

Maqbool T, Raha S, Hoepfner MP, Fogler HS. Modeling the aggregation of asphaltene nanoaggregates in crude oil–precipitant systems. Energy Fuels. 2011;25(4):1585–96. https://doi.org/10.1021/ef1014132.

Mohammadi S, Rashidi F, Mousavi-Dehghani SA, Ghazanfari MH. On the effect of temperature on precipitation and aggregation of

asphaltenes in light live oils. Can J Chem Eng. 2016;94(9):1820–9. https://doi.org/10.1002/cjce.22555.

Mozaffarian M, Dabir B, Sohrabi M, Rassamdana H, Sahimi M. Asphalt flocculation and deposition IV. Dynamic evolution of the heavy organic compounds. Fuel. 1997;76(14–15):1479–90. https://doi.org/10.1016/S0016-2361(97)00151-8.

Rastegari K, Svrcek WY, Yarranton HW. Kinetics of asphaltene flocculation. Ind Eng Chem Res. 2004;43(21):6861–70. https://doi.org/10.1021/ie049594v.

Schaefer DW, Martin JE, Wiltzius P, Cannell DS. Fractal geometry of colloidal aggregates. Phys Rev Lett. 1984;52(26):2371. https://doi.org/10.1103/PhysRevLett.52.2371.

Schramm LL. Emulsions, foams, suspensions, and aerosols: microscience and applications. Hoboken: Wiley; 2014.

Seifried CM, Crawshaw J, Boek ES. Kinetics of asphaltene aggregation in crude oil studied by confocal laser-scanning microscopy. Energy Fuels. 2013;27(4):1865–72. https://doi.org/10.1021/ef301594j.

Sheu EY, Maureen M, Storm DA, DeCanio SJ. Aggregation and kinetics of asphaltenes in organic solvents. Fuel. 1992;71(3):299–302. https://doi.org/10.1016/0016-2361(92)90078-3.

Soulgani BS, Rashtchian D, Tohidi B, Jamialahmadi M. Integrated modelling methods for asphaltene deposition in wellstring. J Jpn Pet Inst. 2009;52(6):322–31. https://doi.org/10.1627/jpi.52.322.

Soulgani BS, Tohidi B, Jamialahmadi M, Rashtchian D. Modeling Formation damage due to asphaltene deposition in the porous media. Energy Fuels. 2011;25(2):753–61. https://doi.org/10.1021/ef101195a.

Speight JG. The chemistry and technology of petroleum. Boca Raton: CRC Press; 2014.

Sun W, Wang W, Gu Y, Xu X, Gong J. Study on the wax/asphaltene aggregation with diffusion limited aggregation model. Fuel. 2017;191:106–13. https://doi.org/10.1016/j.fuel.2016.11.063.

Weitz DA, Oliveria M. Fractal structures formed by kinetic aggregation of aqueous gold colloids. Phys Rev Lett. 1984;52(16):1433. https://doi.org/10.1103/PhysRevLett.52.1433.

Yarranton HW, Masliyah JH. Molar mass distribution and solubility modeling of asphaltenes. AIChE J. 1996;42(12):3533–43. https://doi.org/10.1002/aic.690421222.

Yudin IK, Nikolaenko GL, Gorodetskii EE, Kosov VI, Melikyan VR, Markhashov EL, et al. Mechanisms of asphaltene aggregation in toluene–heptane mixtures. J Pet Sci Eng. 1998a;20(3–4):297–301. https://doi.org/10.1016/S0920-4105(98)00033-3.

Yudin IK, Nikolaenko GL, Gorodetskii EE, Markhashov EL, Agayan VA, Anisimov MA, et al. Crossover kinetics of asphaltene aggregation in hydrocarbon solutions. Physica A. 1998b;251(1–2):235–44. https://doi.org/10.1016/S0378-4371(97)00607-9.